periodica polytechnica

Civil Engineering
56/2 (2012) 185–196
doi: 10.3311/pp.ci.2012-2.05
web: http://www.pp.bme.hu/ci

RESEARCH ARTICLE

Comparison of experimental and analytical results on masonry infilled RC frames for monotonic increasing lateral load

István Haris / *Zsolt* Hortobágyi
Received 2011-11-11, revised 2011-12-12, accepted 2012-01-12

Abstract

The aim of the paper is to give a suggestion to the structural engineers to model masonry infilled reinforced concrete frames. We made several experiments, and developed some numerical models. One question is how to model the infill masonry for monotonic increasing lateral load? Three different numerical models were investigated. The simplest model is the equivalent diagonal strut model, where the masonry wall is replaced by a compressed diagonal strut. The next model is the orthotropic surface model, where the masonry wall is taken into account as a membrane or shell surface. Between the RC frame and the boundary of the surface are modelled with special spring and contact elements. The last model is called "suggested sophisticated model", where the bricks and the mortar layers are separately modelled. The brick is taken into consideration as an orthotropic membrane element, while the mortar layers are substituted with short perpendicular and diagonal equivalent compressed struts. We give the necessary data to the material properties. We suggest a bilinear stress-strain relationship that allows reach the experimental results more accurately than the usage of the material values in accordance with Eurocode 6.

Keywords

masonry infilled RC frames · monotonic increasing lateral load · numerical modelling of infill masonry wall · material characteristics of the masonry infill

István Haris

Budapest University of Technology and Economics, Department of Structural Engineering, 3-9. Műegyetem rkp., fszt. 85, Budapest, H-1111, Hungary
e-mail: haris@vbt.bme.hu

Zsolt Hortobágyi

Budapest University of Technology and Economics, Department of Structural Mechanics, 3-9. Műegyetem rkp., fszt. 63, Budapest, H-1111, Hungary
e-mail: zsolt@hortobagyi.com

1 Introduction

In Hungarian structural design infill masonries are usually considered as non-load bearing, non primary structural elements. Only the concrete frame is assumed to carry horizontal and lateral loads. The most common effect in Hungary, which could be lateral effect during the lifetime of a building according to the valid standard Eurocode 6, is the wind load. Special attention has been nowadays given to the examination on the lateral cyclic horizontal loading, principally on the seismic vulnerability of the masonry infilled concrete frames. Understanding the behaviour of the masonry infilled concrete frames for cyclic lateral loading an experimental research was started at BME in Hungary. Before the first experimental step, different finite element models had been worked out (Haris, Hortobágyi 2007, 2012/2) to describe the behaviour of the infilled frames under lateral loading taking practical aspects into consideration. After it, one-third scale, one-bay, two-storey reinforced concrete (RC) frame specimens were tested in the Structural Laboratory of the Department of Structural Engineering. The first experimental tests and results were engaged in the examination of the monotonic increasing laterally loaded infilled RC frames (Haris, Hortobágyi 2012/2). The preparation and examination of the cyclic lateral loaded specimens are under investigation, and hopefully soon also will be published in another article. The presented results and conclusions will be the basis of the cyclic lateral loaded experiment studies, the effective and useable load histories will be defined according to this article's considerations.

Also the main goal of this article to give a useable method for the designers to how to take into consideration the infill masonry made of "classical" Hungarian solid masonry units and commercially available mortar in everyday practice for monotonic increasing static and quasi-static lateral forces according to Eurocode 6 specify with the nowadays available scientific results.

2 Short review

Many analytical and experimental results showed due to changes in stiffness and mass, dynamic characteristic/response of the whole structure also changes (Magenes, Pampanin 2004;

Bell, Davidson 2001; Puyol et al. 2008; Dincel 2009, Dulácska 2009). The infill masonry has an effect on both global and local failure modes, new and unexpected (by the unfilled frames) and un-designed forms of failure could be appeared (Shing, Mehrabi 2002).

After the investigations of Polyakov (1957) and Holmes (1961), the infill masonry was replaced by an equivalent compressed diagonal strut. Smith (1962, 1966) Smith, Carter (1969) defined the equivalent cross-sectional area of the strut in a closed formula. This method is examined in this article according to the rules of Eurocode 6. Mainstone (1971, 1974) specified the theoretical equations with empirical relations. Because of the imprecision of the elastic theories, from the 70's in order to specify the methods the attention principally was paid to theories of plasticity (Wood 1978; May 1981; Dawe, Seah 1989). Finally Saneinejad and Hobbs (1995) published an article included the main results, which are taken the pillar of this theme by nowadays researchers. Shing and Mehrabi (2002) defined the most common five failure modes and the effective ultimate load carrying capacity of the weakly and strongly masonry-infilled frames. By the evolution of the softwares using in structural design process many analytical and numerical models and results (Lourenço et al. 2006, Mehrabi et al. 1996, Haris, Hortobágyi 2012/2) were published. Above all many experimental results also were presented in connection with the masonry infilled steel frames (Seah 1998; Tasnimi, Mohebkhah 2011) and concrete frames (Calvi et al. 2004, Murty, Jain 2000; Braz Cesar et al. 2008, Baran, Sevil 2010).

3 Experimental study

3.1 Test frames

In the experimental part of the study one-third scale, one-bay, two-storey reinforced concrete (RC) frames were used as specimens in the execution of the tests (Haris, Hortobágyi 2012/1). On the whole 9 specimens were tested; the dimensions and the reinforcements of the concrete skeleton can be seen in Figure 1. The ratio of one storey infill height (h) and length (ℓ) h/ℓ is 0.595.

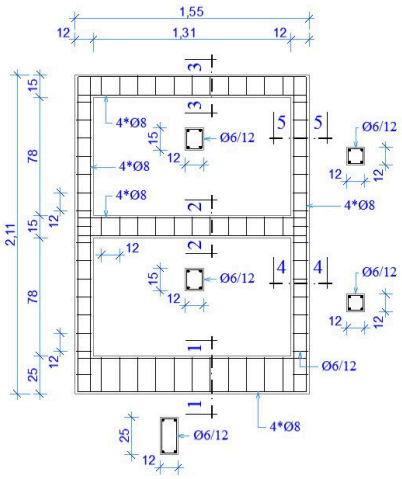

Fig. 1. Dimensions and reinforcements of the test frames

9 specimens were investigated, as it can be seen in Table 1.

Tab. 1. Investigated test frames

Sign	Infill	Mortar	Pieces
K0	without infill	-	3
Km1	infilled	Baumit M30	3
Km2	infilled	Baumit M100	3

The concrete skeletons were prefabricated in a concrete factory. Test frames have intentionally been designed with most common deficiencies observed in the practice, such as restraint connections between beams and columns. The bending stiffness of the columns was so much smaller than the bending stiffness of the beams, together with common characteristics of materials (reinforcement and concrete) were used, see in Table 2.

Tab. 2. Classifications of the used materials

Used materials	Classifications	
Concrete	C20/25	f_{ck}= 20 N/mm^2
Steel reinforcement	S500B	f_{yk}= 500 N/mm^2

The RC frame was posteriorly infilled in the laboratory. The used masonry unit was the so-called "classic" solid small brick with dimensions 6.5*12*25 cm, and each of the elements were cutted into three uniform pieces to take into consideration the scale of the RC test frame, see in Figure 2.

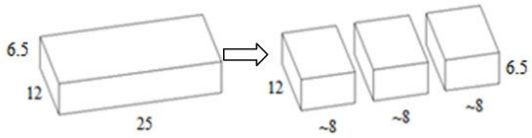

(a) 6.5*12*25 cm (b) 6.5*12*8 cm

Fig. 2. The "classic" solid small brick in Hungary

The mean compressive strength of the masonry unit (data of the factory) is f_k= 10 N/mm^2. The normalized compressive strength of the cutted units (6.5*12*8) was calculated by EC6, that is f_b= 8.57 kN/mm^2. The average thickness of both mortar layers was about 3-3.5 mm, and the whole surface was covered with mortar. The RC frames were infilled from the top to the bottom, namely first the upper storey was infilled, then the lower one.

Two different mortars were used in the experiments, see in Table 3.

Both of the main values of the material characteristic were checked in the laboratory, such as the concrete, the reinforcement and the masonry unit. The difference between the designed and the measured values were similar with each other, except the compression strength of the mortar, see in Table 4.

The infill masonry was continually chocked to the concrete surface with using steel plates, see on Figure 3.

Tab. 3. Classifications of the designed mortars

Classification of mortar	Compr. strength f_m [N/mm^2]
Baumit M30 (M3)	3
Baumit M100 (M10)	10

Tab. 4. Classifications of the executed mortars

Sign of specimen	Executed Class. f_m [N/mm^2]
Km1 - Sp.1.	2,3
Km1 - Sp.2.	2,7
Km1 - Sp.3.	3,3
Km2 - Sp.1.	9,3
Km2 - Sp.2.	8,0
Km2 - Sp.3.	8,5

3.2 Loading and supporting system

The one-bay, two-storey reinforced concrete (RC) frames were fixed by complementary steel structures to the concrete slab. The static test loading consisted lateral uniaxial, monotonic increasing loading (V) at the top beam of the frame besides constant (100 kN) vertical load applied on both columns, see on Figure 4. All of the loadings were applied by using hydraulic jack. A very rigid external steel frame attached to the specimen was used to prevent any out-of-plane deformations, see also on Figure 4.

3.3 Deformation measurements

All deformations were measured by inductive displacement transducers, such as the top drifting under the centre line of the top beam by Type W100 (HBM), the relative displacements (1e-8e) between the masonry and the concrete by Type W1 and W1/2, the buckling displacements (1k-5k) normal to the equivalent diagonal strut by Type W1. All the electrical signs were detected and the signals were processed by software and PC (2 pieces of Spyder8), see on Figure 5.

3.4 Experimental results

At the followings the test frames are evaluated in terms of load - top displacement. A typical load-top displacement curve shows up at Figure 6.

The results of the two test series with the different mortars are shown at Figure 7.

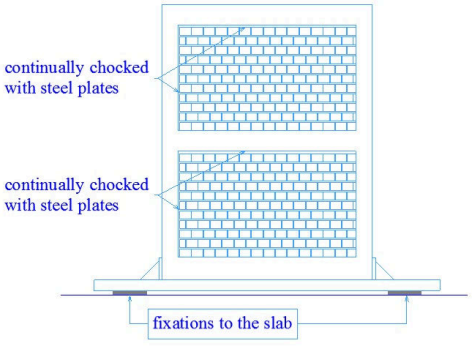

Fig. 3. The infilled frame specimen

At specimen Km1-Sp.3. the final failure was not eventuate because the test frame was retained for educational aims at the university. All of the other frames were loaded up to the collapse. After the infilled test frame had not been able to carry higher horizontal forces or had been sliding horizontally under constant force, the specimen was started to unload. At specimen Km1-Sp.2. and Km2-Sp.2. execution problem was occurred. The steel reinforcements in the right concrete column were in wrong position at the middle beam-column connection, so the shear resistance of the concrete element was significantly decreased. After the first diagonal cracks were appeared on the infill, when the masonry units had been sliced, a very quickly shear cracking were observed, that is why the experimental results are smaller than the other ones. The point, when the first diagonal main cracks evolve, is called by the scientific literature as the "yield point" of the masonry, see on Figure 8.

To able to make the comparison with the results of the different numerical models, at the main measured external lateral load points (yield force of the masonry infill and peak load of the infilled frame) the top displacements of the infilled frames are the followings, see in Table 4.

Tab. 5. Measured top displacements at infilled frames (Km1-Sp.3. was not tested up to collapse as it was mentioned before, the value of the peak load of Km2-Sp.2. was lower than V=92 kN because of the execution problem)

Sign of spec.	Measured top displacement [mm]	
	V= 82 kN	V= peak load
Km1-Sp.1.	7.65	37.4
Km1-Sp.2.	5.92	30.3
Km1-Sp.3.	4.10	-
	V= 92 kN	V= peak load
Km2-Sp.1.	10.61	28.76
Km2-Sp.2.	-	25.04
Km2-Sp.3.	12.37	31.82

Without striving for completeness the failures of the specimens are presented below, Figure 9.

4 Analytical study

In this part of the article numerical results of three different finite element (Haris, Hortobágyi 2012/2) models will be described according to the specifications of Eurocode 6.

4.1 Models of the infill masonry wall

To describe the behaviour of the infilled frames under lateral loading taking practical aspects into consideration Haris and Hortobágyi (2012/2) were introduced three different FEM models.

The static scheme of the models is shown in Figure 10.

4.1.1 Equivalent diagonal compressed strut model

The cast-in-situ reinforced concrete structures (columns, beams) are taken into consideration with their actual geometric and material characteristics in the calculation, whereas infill

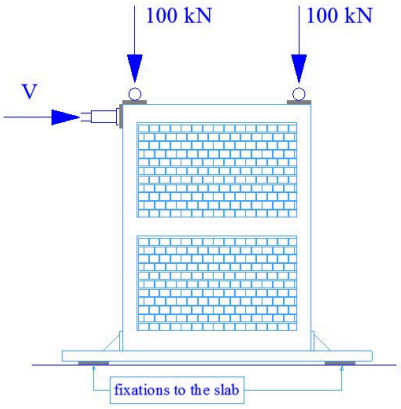

(a) Scheme of the test frame

(b) Hydraulic jacks on an unfilled frame

Fig. 4. Loading system

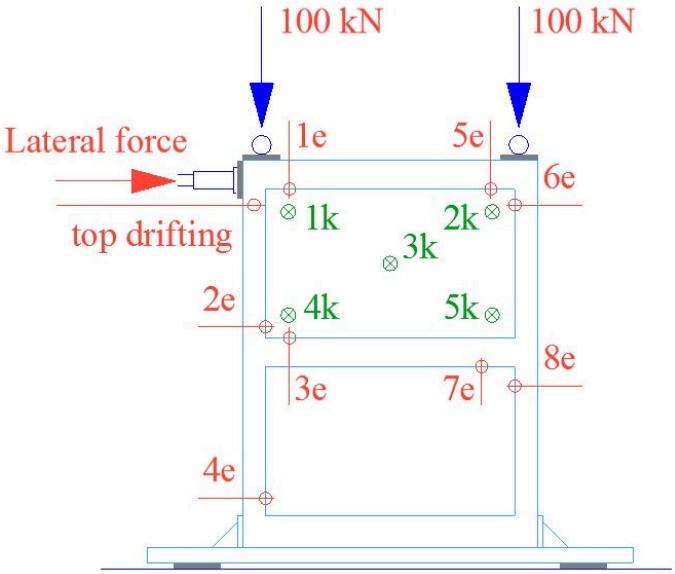

(a) Measurement points on the test frame

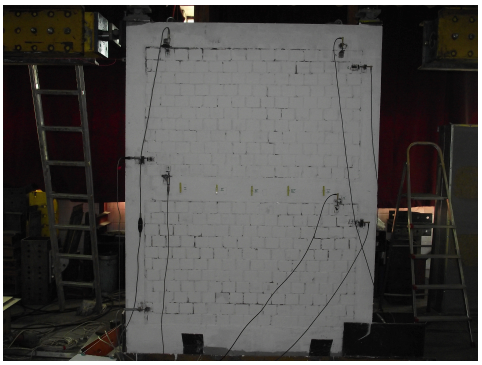

(b) Set-up of the measurement (front)

(c) Back-side of the specimen

Fig. 5. Displacement measurement

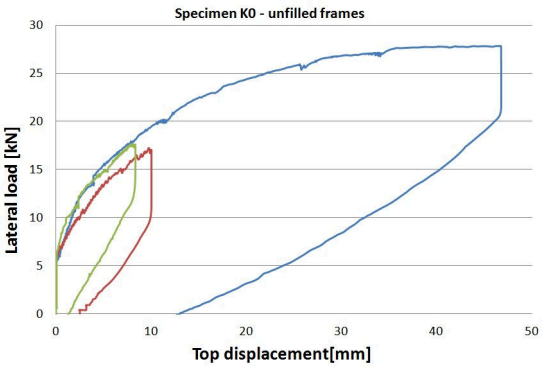

Fig. 6. Load-top displacement curves of the unfilled test frames (two of the specimens were only loaded up to the first concrete crack, not to the collapse)

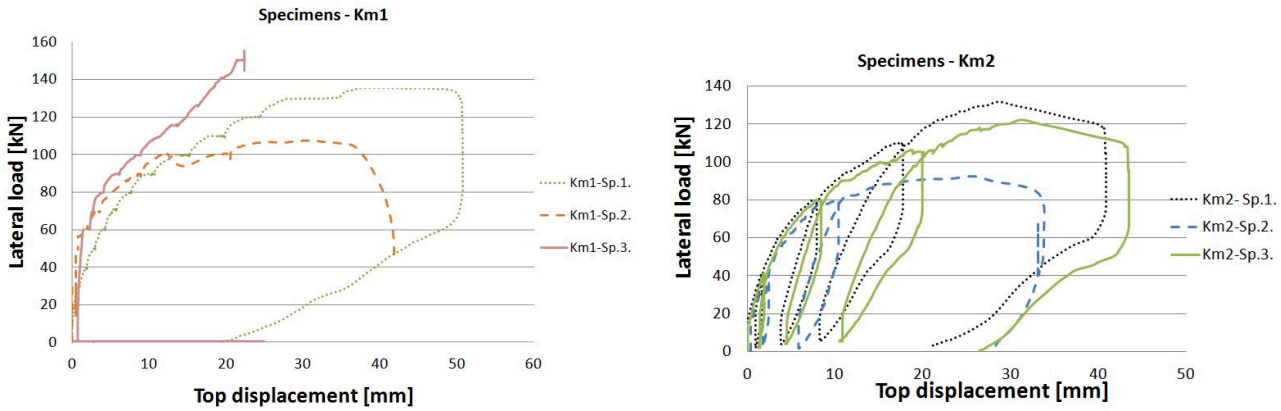

(a) Infilled frames using mortar M3

(b) Infilled frames using mortar M10

Fig. 7. Load-top displacement curve of the infilled test frames

(a) Typical cracks on specimen

(b) Typical cracks on specimen

Fig. 8. Typical failure modes, cracks of the specimens

masonries are modelled by a so-called equivalent diagonal compressed strut, Figure 10 (a). The cross-sectional parameters of the equivalent strut should be calculated with the following formulas (Smith 1962, 1966, Smith and Carter 1969):

$$a_{infill} = 0.175(\lambda h_{col})^{-0.4} d \tag{1}$$

$$\lambda = \sqrt[4]{\frac{E_{infill} b_w \sin(2\beta_s)}{4EIh_{inf}}} \tag{2}$$

where a_{infill} is the effective width of the equivalent diagonal strut, λ is a dimensionless parameter, h_{col} is the height of the concrete column between the centrelines of the beams in one storey, d is the diagonal length of the infill masonry, E_{infill} is the Young's modulus of the infill, b_w is thickness of the masonry, β_s is the angle of the diagonal, E is the Young's modulus of the concrete column, I is the moment inertia of the concrete column, h_{inf} is the height of the infill masonry.

In this article different material characteristics will be introduced in accordance with the rules of EC6 to calculate the deformations more realistic, see chapter 4.2.

4.1.2 Mesh surface model

In this case the model of the concrete elements is the same, but the masonry infill is modelled by orthotropic shell (or membrane) elements, and the connection between concrete and masonry is taken into account by nonlinear spring and contact elements (Haris, Hortobágyi 2012/2), Figure 10 (b) and Figure 11.

The behaviour of the spring is specified with a spring constant (ρ), what can be calculated with Formula (3):

$$\rho_{sping} = E_m \frac{t_{infill} l_{spring}}{v_{mortar}} \tag{3}$$

where E_m is the Young's modulus of mortar, approximately now could be substituted with $E_{infill;}$ see at (6), t_{infill} is the thickness of the infill masonry could be replaced with 0.8*b_w; l_{spring} is the distance between spring elements in the FEM model, v_{mortar} is the thickness of the mortar between the brick elements and the concrete skeleton.

The different material characteristics of the infill masonry will be described in the next Chapter.

4.1.3 Suggested sophisticated model

The infill masonry panel is modelled by modelling separated each brick elements and mortar layers, Figure 10 (c). A brick element is taken into consideration as an orthotropic shell or membrane element with its Young's modulus, the strengths in two perpendicular directions and the Poisson's ratio. To model the nonlinear connection between the brick element and the mortar, the mortar layers are replaced with two equivalent compressed struts (Haris, Hortobágyi 2012/2), Figure 12.

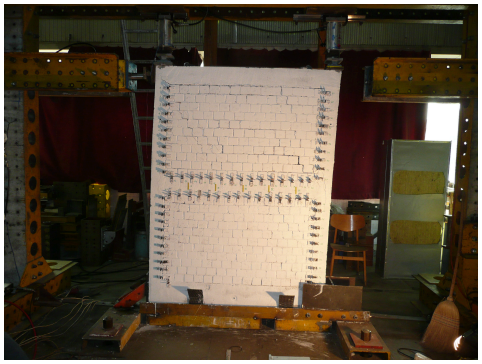

(a) Specimen Km1 - Sp.1.

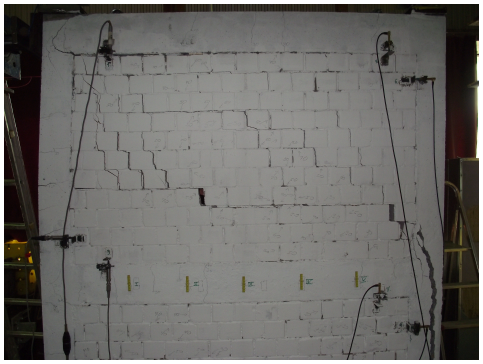

(b) Specimen Km1 - Sp.2.

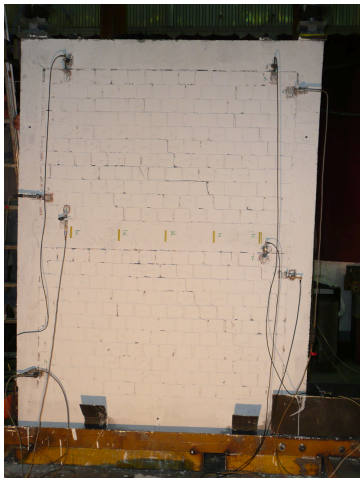

(c) Specimen Km1 - Sp.3.

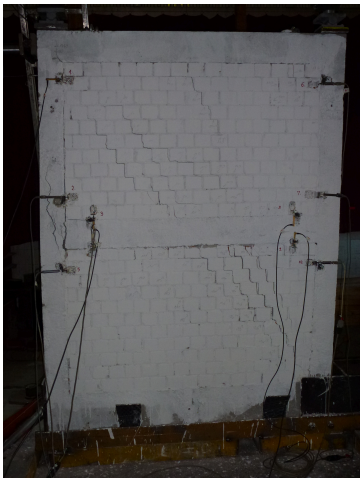

(d) Specimen Km2 - Sp.1.

(e) Specimen Km2 - Sp.2.

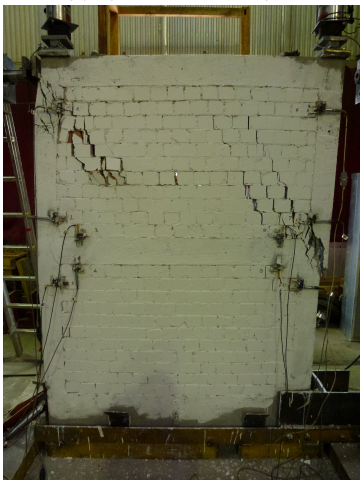

(f) Specimen Km2 - Sp.3.

Fig. 9. The failures of the infilled test frames

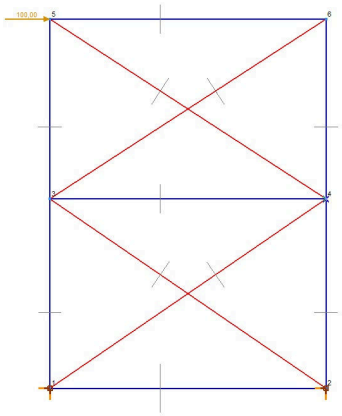

(a) Equivalent diagonal strut model (Smith. 1962, 1966, Smith, Carter 1969)

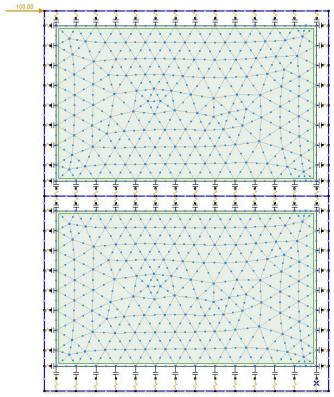

(b) Mesh surface model

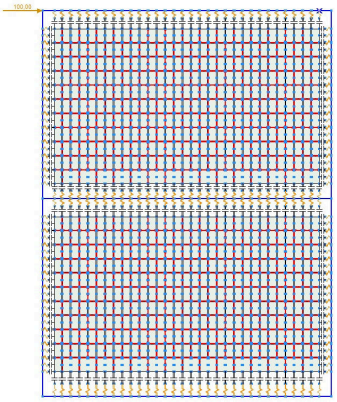

(c) New suggested model with equivalent struts of the mortar

Fig. 10. Static scheme of the models of the masonry infilled RC frames

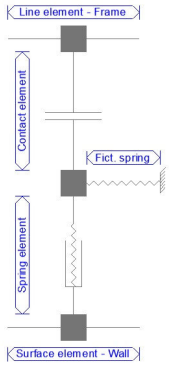

(a) Static scheme of connection

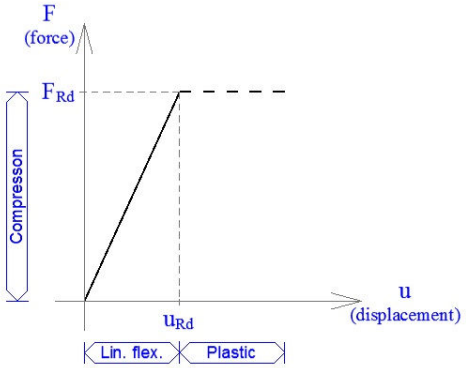

(b) Joint behaviour of the connection

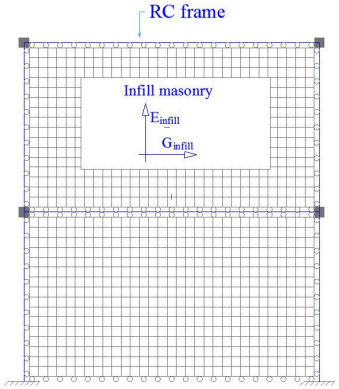

(c) Orthotropic shell model

Fig. 11. The build-up of the orthotropic surface model

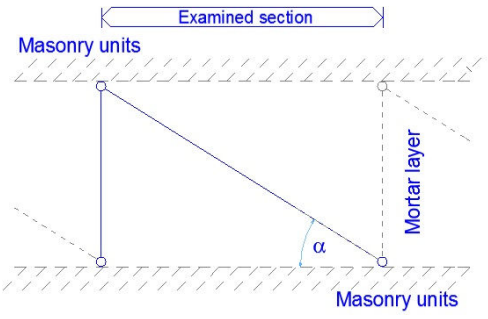

(a) Static scheme

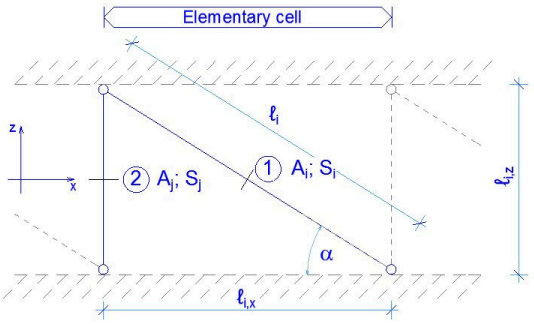

(b) Equivalent struts of the mortar

Fig. 12. The build-up of the equivalent strut model of the mortar

The formulas were given (Haris and Hortobágyi 2012/2) to calculate the equivalent normal stiffness *(EA)* of the struts, Formula (4); (5); (6) and (7).

$$A_i = \frac{f_{vd}\ell_i v_{inf}}{f_{md}} \tag{4}$$

$$A_j = \ell_{i,x} v_{inf} - A_i \frac{\ell_{i,z}}{l_i} \tag{5}$$

$$E_j = \frac{E_m \ell_{i,x} v_{inf}}{A_j} \tag{6}$$

$$\frac{1}{E_i} = \frac{E_i}{E_m v_{inf}} \left[\frac{\ell_{i,z}\ell_{i,x}}{\ell_i^3} 2(1+\nu_m) - \frac{\ell_{i,z}^3}{\ell_i^3 \ell_{i,x}} \right] \tag{7}$$

where A_i and A_j are the cross-sectional area of the equivalent struts, E_i and E_j are the Young's modulus of the equivalent struts, f_{md} is the design value of the compression strength of the mortar, f_{vd} is the design value of the shear strength of the mortar, v_{inf} is the thickness of the masonry, see ℓ_i and $\ell_{i,x}$; $\ell_{i,z}$ on Figure 11, E_m is the Young's modulus of the mortar, ν_m is the Poisson's ratio of the masonry unit

By using this method "only" the separated elements' material data of the masonry infilled RC frame are sufficient for the calculation, such as the Young's modulus, Poisson's ratio and the value of different strength (shear, compression) of the mortar, the masonry unit and the concrete skeleton. To get the guarantied and probably well-tested material data of the masonry unit and the mortar from the Factory could be easier and calculable than appreciate the executed quality for a designer. In case of doubt the numerical values of the material characteristics can be determine with the help of experimental results (Fódi, 2011).

4.2 Material characteristics of the masonry infill

The material characteristics taken into consideration must be specified in accordance with rules of EN 1996-1-1 (Eurocode 6): Design of masonry structures. The specifications for unreinforced masonries are the followings:

- determination of the characteristic compressive strength perpendicular to bed joints (using general purpose mortar):

$$f_k = K f_b^{0.7} f_m^{0.3} \tag{8}$$

  where the value of K depends on the density of the used mortar and the type of the masonry units, f_b is the normalized compressive strength of the masonry units in N/mm^2, f_m is the specified compressive strength of the general purpose mortar in N/mm^2.

- the initial Young's modulus of the masonry for use in the structural analysis, if test results are not available accordance with standard EN 1052-1 (*Methods of test for masonry*) (this is the most common in design practice):

$$E_{ini} = 1000 f_k \tag{9}$$

- when the modulus of elasticity is used in calculations relating to the serviceability limit state a secant modulus is suggested to calculate with:

$$E_{infill} = 0.6 \cdot 1000 f_k \tag{10}$$

- the shear modulus:

$$G_{infill} = 0.40 E_{infill} \tag{11}$$

  where f_d is the design value of the compressive strength of the unreinforced masonry in N/mm^2, σ is the stress and ε is the strain.

The stress-strain relationships for masonry are shown in Figure 13. according to EC6.

For design the masonry according to EC6 the $\sigma - \varepsilon$ curve consists of an elastic and a perfect plastic section, no further information are available for serviceability limit states in the code.

These formulas and $\sigma - \varepsilon$ curve are securely short for the realistic design procedure of the structure, so the material data of the masonry infill must be specified. El-Dakhakhni et al. (2003) suggested that the Young's modulus in diagonal (β) direction shall be calculated with Formula (12):

$$\frac{1}{E_{infill.\beta}} = \frac{1}{E_{infill.0}} \cos^4(\beta) + \left[-\frac{2\nu_{0-90}}{E_{infill.0}} + \frac{1}{G_{infill}} \right] \cos^2(\beta)\sin^2(\beta) + \frac{1}{E_{infill.90}} \sin^4(\beta) \tag{12}$$

where $E_{infill.0}$ and $E_{infill.90}$ are Young's modulus of the infill masonry in the direction to parallel and normal to mortar bed joints, $E_{infill.90}$ is equal to (10), ν_{0-90} is Poisson's ratio, G_{infill} is shear modulus. $E_{infill.0}$ could be taken as half of $E_{infill.90}$, and ν_{0-90}= 0.25.

The value of the ultimate strength of the infill masonry in the direction of the diagonal (β), $f_{infill-\beta}$ was suggested to calculate with Formula (13) (Hamid and Drysdale 1980):

$$f_{infill-\beta} = 0.7 \cdot f_{infill-90}. \tag{13}$$

Change $f_{infill-90}$ with (8) the following shall be used according to Eurocode:

$$f_{infill-\beta} = 0.7 \cdot f_k. \tag{14}$$

Non-linear finite element analysis conducted by Saneinejad and Hobbs (1995) suggested that the secant stiffness of the infilled frames at the peak load to be half of the initial stiffness. This suggestion can be adapted to the calculation of the Young's modulus in Formula (15):

$$E_{infill-peak} = 0.5 \cdot E_{infill.\beta}. \tag{15}$$

According to EC6 specified with the above mentioned suggestions of the scientific literature, we suggest to use a new σ-ε diagram on the serviceability (displacements) designing method of the lateral loaded masonry infills. Accordance with Hamid and Drysdale (1980) and with Formula (14) a bilinear relation stress-strain diagram could be defined (El-Dakhakhani et

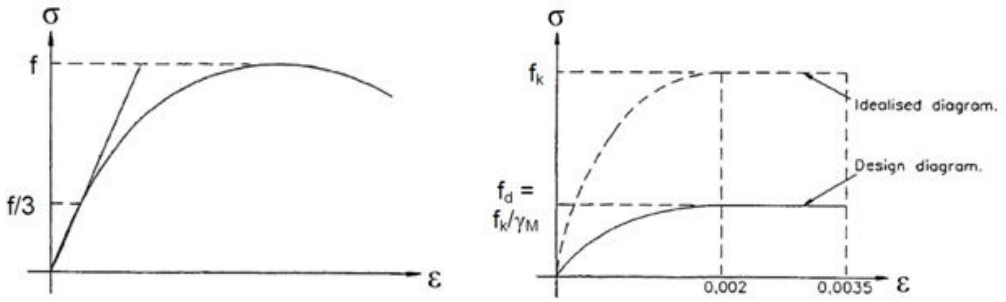

(a) General shape of a stress-strain relationship

(b) Stress-strain relationship for the design

Fig. 13. Stress-strain relationship according to EC6

al. 2003). Up to the yield point (the point of the first diagonal crack in the masonry) an elastic section could be defined in accordance with EC6, after it following the second linear line, the perfect plasticity should be neglected, a monotonic linear decreasing section is suggested, see in Figure 14.

$$f_{yield} = f_{infill-\beta} = 0.7 \cdot f_k. \tag{16}$$

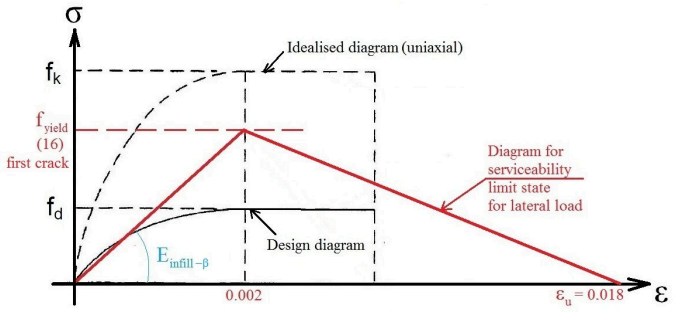

Fig. 14. Suggested stress-strain relationship to modelling the displacements of the masonry infill for lateral load at least in biaxial stress state

Taken into consideration the suggestions at cycling loading of Baran and Sevil (2010), the yield stress of the masonry infill could be calculated by using Equation (17):

$$F_{yield} = \gamma f_{yield} \alpha_{infill} b_w. \tag{17}$$

where γ is a variable due to the column axial load effect on the ultimate load carrying capacity of the equivalent compressed diagonal strut. γ was given by Baran and Sevil (2010) by Formula (18):

$$\gamma = 1 + \left(\frac{N}{N_0}\right) \leq 1.3 \tag{18}$$

where N is the effective axial load on the column, N_0 is the ultimate load carrying capacity of the concrete column.

4.3 Brief introduction to the FEM software applied

In the present case, modelling was performed using the FEM software AxisVM 11.

The software applies isoparametric plain quadrilateral (8/9-node) or triangular (6-node) elements to model surfaces. Their shape functions are of the second degree. 3-node rib elements are recommended for modelling linear elements as they also take the impact of shear deformations into account in the course of calculation.

5 Comparison of analytical and experimental results

The numerical calculations in accordance with EC6 were made, where the infill masonry was modelled by equivalent diagonal strut and shell surface, such as the other (mesh model and suggested sophisticated model) proposed analytical methods with the suggested material characteristics.

The curves signed “EC6 strut” and “EC6 surface” were calculated by the material characteristics according to EC6, where infill masonry were modelled by equivalent compressed strut (Figure 9 (a)) and by orthotropic shells (Figure 9 (b)), see at Chapter 4.1. Both curves named “Surface model” (Figure 9 (b)) and “Soph. model” (Figure 9 (c)) were calculated by the model methods were shown in Chapter 4.1 (Haris, Hortobágyi 2012/2), in accordance with the material characteristics are shown at Figure 14.

The comparison of the experimental and the analytical results could be seen in Figure 15 and 16, such as the comparison of the above mentioned model methods with the material values in accordance with EC6 and with the suggested strain-stress relationship.

Evaluation of the comparison of the executed experimental and analytical tests:

- Km1-Sp.1.: the coincidence of the experimental and the analytical results is very good using the suggested bilinear σ-ε diagram for the infill masonry and the suggested sophisticated FEM model.
- Km1-Sp.2.: up to the yield point of the masonry there is a little deviance between the curves, but after evolving the first diagonal cracks in the masonry both of the calculated curves shows unacceptable differences to the experimental results. It can be explained with the execution problems of the concrete skeleton.
- Km1-Sp.3.: the coincidence of the experimental and the analytical results is also very good using the suggested bilinear σ-ε diagram for the infill masonry and the suggested sophisticated FEM model up to the end of the experimental test, which was interrupted.

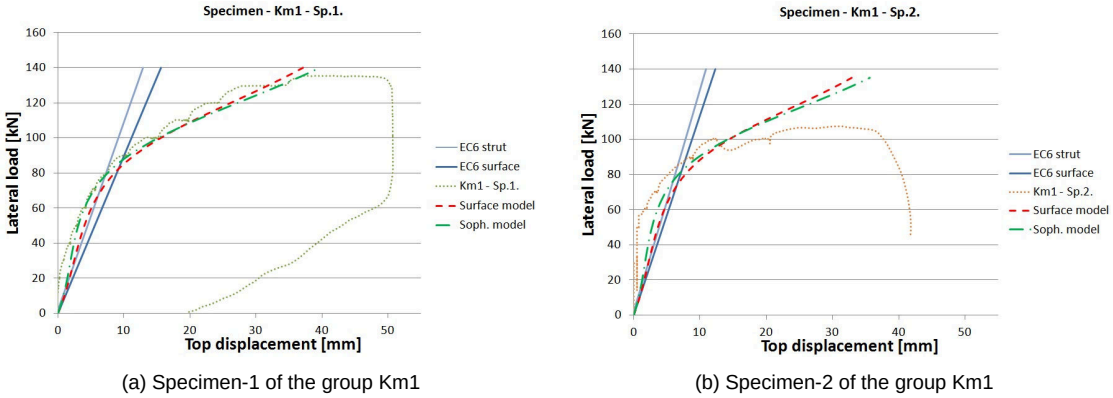

(a) Specimen-1 of the group Km1

(b) Specimen-2 of the group Km1

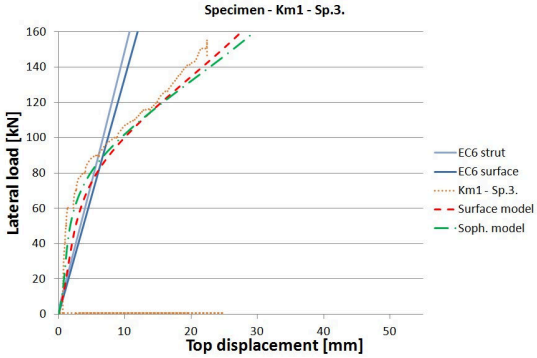

(c) Specimen-3 of the group Km1

Fig. 15. Comparison of experimental and analytical results, Specimens Km1 group

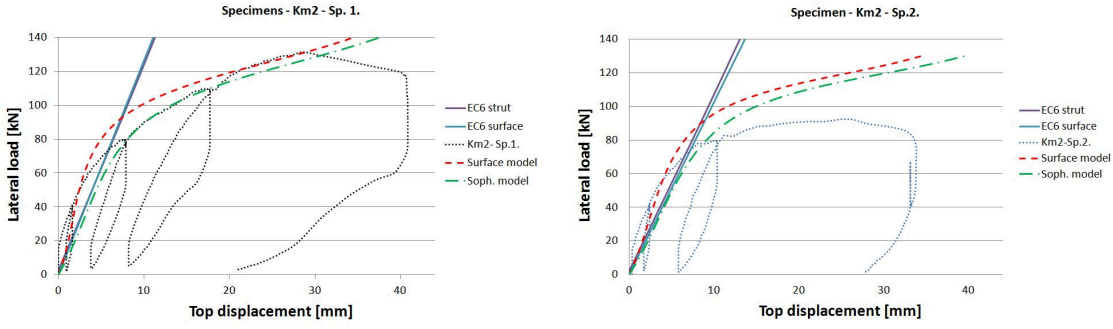

(a) Specimen-1 of the group Km2

(b) Specimen-2 of the group Km2

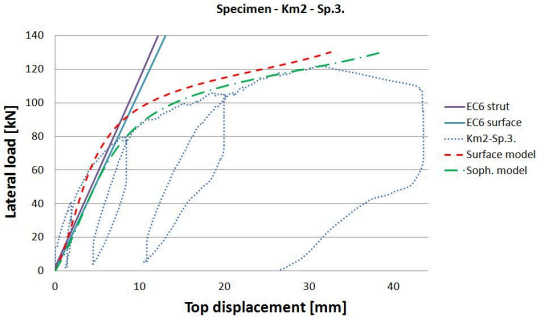

(c) Specimen-3 of the group Km2

Fig. 16. Comparison of experimental and analytical results, Specimens Km2 group

As it could be seen on Figure 15, that the specimens were loaded in echelon, while the numerical results do not show the up- and unloading "steps".

Evaluation of the comparison of the executed experimental and analytical tests:

- Km2-Sp.1.: the coincidence of the experimental and the analytical results is very good using the suggested bilinear σ-ε diagram for the infill masonry and the suggested sophisticated FEM model.
- Km2-Sp.2.: in the first section of the curve there is a little deviance between the measured and calculated curves, but after it due to the execution problems of the concrete skeleton usable conclusion cannot be made.
- Km2-Sp.3.: the coincidence of the experimental and the analytical results is also very good using the suggested bilinear σ-ε diagram for the infill masonry and the suggested sophisticated FEM model.

Maybe better, more coincidence numerical results can be shown with a trilinear σ-ε curve, it can be the theme of further investigations.

6 Conclusions

The conclusions made below are based on the limited data of the experimental tests and numerical studies of the masonry infilled RC frames. The numerical results of three different finite element models of masonry infilled reinforced concrete frames were compared with experimental results.

The two-storey, one-bay RC test frames showed similar behaviour, especially the initial stiffness of the frames, the yield point of the masonry infills and the peak lateral loads were close, except two specimens, where execution problems were occurred. But the initial section of the response curves of these test frames, up to the yield force of the masonry infill, were also close, only the peak loads and collapse displacements were smaller, this can be owing to the quality of the construction of the RC frames.

With the different proposed methods the deviations of the estimation of the top displacements of the test frames show quite big differences. By the investigation of the above shown Figures the following statements could be made:

- by the equivalent strut model and the surface model with the material data of EC6, the difference between the experimental and numerical results are more than 20% up to the yield force of the masonry infill, moreover after it the calculable top displacements are unacceptably incorrect,
- by using the introduced "Mesh surface model" with spring-contact FEM elements modelling the relationship between concrete and masonry, and also using the suggested bilinear $\sigma - \varepsilon$ curve for the masonry infill, the difference between the experimental and numerical results are under 20 % either up to the yield force of the masonry and after it,
- by applying the method of the shown "Suggested sophisticated model" with the equivalent sheared and compressed struts replaced the mortar layer, the computable differences are under 10 % between the numerical and the experimental results before the first diagonal cracks are evolving, after the yield point of the infill masonry the differences are under 15 %, but the up- and unloading periods were not modelled.

Using the material data according to EC6 in equivalent strut model and in mesh surface model is not suggested, because the numerical results shows quite big (~40%) difference in top displacements up to the yield force of the masonry. The computable top displacements after the yield point of the infill are incorrect, and not able to be suggested to use in design method.

By using the proposed bilinear material characteristics of the infill masonry in orthotropic surface model with the suggested connection model between the concrete and the masonry infill gave safe and reliable results to the behaviour of the infilled RC frames. Although this proposed method is a little bit more difficulty, closer results can be presented for the top displacements, already for the stage after the yield point of the masonry.

The third shown model, the suggested sophisticated model, is much more complicated, even so is usable in design practice. This model gave the closest numerical results in top displacements to the experimental results. The differences between the experimental and analytical results were under 10-15% at the stage before and after yield point of the masonry infill.

Using the proposed bilinear σ-ε curve of the masonry infill, which is based on EC6, in an orthotropic surface model with the presented connection elements, or using the suggested sophisticated model with the equivalent struts of the mortar layer shows good correlation with the test results. By these ways the top displacements of the masonry infilled RC frames can be calculated in good approximation also after the yield point of the infill masonry, and are already usable in the structural engineering none the less the complexity of the methods.

Acknowledgements

The authors would like to express their grateful thanks to the colleagues in the Laboratory of the Budapest University of Technology and Economics. The study presented in this article was sponsored by TÁMOP 4.2.1/B-09/1/KMR-2010-0002. Their funding is gratefully acknowledged.

References

1 *Eurocode 6 EN 1996-1-1:2009, Design of Masonry Structures*, 2009. European standard.

2 **Baran M., Sevil T.**, *Analytical and Experimental Studies on Infilled RC Frames*, Int. Journal of the Physical Sciences **5** (2010), no. 13, 1981–1998.

3 **Bell D. K., Davidson B. J.**, *Evaluation of Earthquake Risk Buildings with Masonry Infill Panels*, New Zealand Society for Earthquake Engineering Inc. 2001 Conference, 2001, pp. Paper No. 4.02.01.

4 **Braz-Cesar M. T, Oliveira D., Barros R. C.**, *Comparison of Cyclic Response of Reinforced Concrete Infilled Frames with Experimental Results*,

14th World Conference on Earthquake Engineering (Beijing, China, October 12-17, 2008).

5 **Calvi M. G., Bolognini D., Penna A.**, *Seismic Performance of Masonry-Infilled RC Frames: Benefits of Slight Reinforcements*, SÍSMICA 2004-6 Congresso National de Sismologia e Engenharia Sísmica, 2004, pp. 253–276, http://www.civil.uminho.pt/masonry/Publications/Sismica_2004/253-276_G_Michele_Calvi.pdf.

6 **Dawe J. L., Seah C. K.**, *Behaviour of masonry infilled steel frames*, Canadian Journal of Civil Engineerings **16** (1989), no. 6, 865–876.

7 **Dincel B.**, *The Roles of Masonry Infill Wall sin an Earthquake*, 2009, http://www.dincelconstructionsystem.com. Dincel Contruction System, Paramatta, Australia.

8 **Dulácska E.**, *Földrengés elleni védelem, egyszerű tervezés az Eurocode 8 alapján (in Hungarian)(Earthquake protection, simple design based on Eurocode 8)*, 2009. Practical guide.

9 **Fódi A.**, *Effects influencing the compressive strength of a solid, fired clay brick*, Periodica Polytechnica - Civil Engineering **55** (2011), no. 2, 117–128, http://www.pp.bme.hu/ci/2011_2/pdf/ci2011_2_04.pdf.

10 **El-Dakhakhni W. W., Elgaaly M., Hamid A. A.**, *Three-Strut Model for Concrete Masonry-Infilled Steel Frames*, Journal of Structural Engineering **129** (February 2003), no. 2, 177–185.

11 **Hamid A. A., Drysdale R. G.**, *Concrete Masonry under Combined Shear and Compression Along the Mortar Joints*, ACI Journal **77** (1980), no. 5, 314–320.

12 **Haris I., Hortobágyi Zs.**, *Modelling cast-in-situ reinforced concrete frame stiffened by masonry wall using FEM software*, Central Europen Congress on Concrete Engineering (Visegrád, Hungary, September 17-18, 2007), Proceedings of CCC2007 (fib), 2007, pp. 469–474.

13 **Haris I., Hortobágyi Zs.**, *Experimental research of masonry infilled frames for static load (in English translation)*, Concrete Structures (fib) **14** (2012), no. 1, 25–30. Budapest, Hungary,.

14 **Haris I., Hortobágyi Zs.**, *Different FEM models of Reinforced Concrete Frames Stiffened by Infill Masonry for Lateral Loads*, Periodica Polytechnica - Civil Engineering **56** (2012), no. 1, 25–34.

15 **Holmes M.**, *Steel frames with brickwork and concrete infilling*, Institution of Civil Engineers (London, England, 1961), ICE Proceedings, Vol. 19, 1961, pp. 473–478. E-ISSN: 1753-7789.

16 **Magenes G., Pampanin S.**, *Seismic Response of Gravity-load design frames with masonry infills*, 13th World Conference on Earthquake Engineering (Vancouver B.C. Canada, August 1-6, 2004), proceedings, 2004. Paper No. 4004.

17 **Mainstone R. J.**, *On the stiffness and strength of infilled frames*, Proc. Inst. Civ. Eng., Struct. Build., Vol. 49, Instn. of Civil Engrs., London, EnglandR, 1971, pp. 57–90. Paper 7360S.

18 **Mainstone R. J.**, *Supplementary note on the stiffness and strength of infilled frames*, Build. Res. Establishment, London, England, 1974. Current Paper CP13/74.

19 **May I. M.**, *Determination of collapse loads for unreinforced panels with and without openings*, Proceedings of Instn. of Civil Engrs., Vol. 71, London, England, 1981, pp. 215–233.

20 **Mehrabi A. B., Shing P. B., Schuller M. P., Noland J. L.**, *Experimental Evaluation of masonry-infilled RC frames*, Journal of Structural Engineering (ASCE) **122** (1996), no. 3, 228–237. ISSN 07339445. ISBN 07339445.

21 **Murty C. V. R., Jain S. K.**, *Beneficial influence of masonry infill walls on seismic performance of rc frame buildings*, 12th World Conference on Earthquake Engineering (Auckland, New Zealand, January 2000).

22 **Lourenço P. B., Alvaregna R. C., Silva R. M.**, *Validation of a Simplified Model for the Design of Masonry Infilled Frames*, Masonry International (2006), 15–26. ISSN 0950-2289. 19:1.

23 **Polyakov S. V.**, *Masonry in Framed Buildings; An Investigations into the Strength and Stiffness of Masonry Infilling* (1957). Moscow (In English translation).

24 **Puglisi M., Uzcategui M., López J. F.**, *Modelling of masonry of infilled frames, Part I: The Plastic Concentrator*, Elsevier Engineering Structures **31** (2009), 113–118.

25 **Puyol S., Benavent-Client A., Rodriguez M. E., Smith-Pardo J. P.**, *Masonry Infill Walls: An Effective Alternative for Seismic Strengthening of Low-rise Reinforced Concrete Building Structures*, 14th World Conference on Earthquake Engineering (Beijing, China, October 12-17, 2008), 2008.

26 **Saneinejad A., Hobbs B.**, *Inelastic Design of Infilled Frames*, Journal of Structural Engineering **121** (1995), no. 4. Paper No. 6682.

27 **Seah C. K.**, *Universal Approach for the Analysis and Design of Masonry-infilled Frame Structures*, PhD. Thesis, University of New Brunswick, Canada, 1998.

28 **Shing P. B, Mehrabi A. B.**, *Behaviour and Analysis of Masonry-infilled Frames*, Progress in Structural Engineering and Materials **4** (2002), no. 3, 320–331.

29 **Smith S. B.**, *Lateral stiffness of infilled frames*, Journal of the Structural Division, ASCE **88** (1962), 183–199.

30 **Smith S. B.**, *Behaviour of square infilled frames*, Journal of the Structural Division, ASCE **92** (1966), 381–403.

31 **Smith S. B., Carter C.**, *A method of analysis for infilled frames*, Proc. of Instn. of Civ. Engrs., Vol. 44, 1969, pp. 31–48. E-ISSN: 1753-7789.

32 **Tasnimi A. A., Mohebkhah A.**, *Investigation on the behaviour of brick infilled steel frames with openings, experimental and analytical approaches*, Engineering Structures **33** (2011), no. 3, 968–980.

33 **Wood R. H.**, *Plastic composite action and collapse design of unreinforced shear wall panels in frames*, Proceedings of Instn. of Civil Engrs., Vol. 65, London, England, 1978, pp. 381–411.